Expression of Slit and Robo During Remodeling of Corticospinal Tract in Cervical Spinal Cord in Middle Cerebral Artery Occlusion Rats

Zhenhao Ying
Shandong University of Traditional Chinese Medicine
Junxuan Wu
Shandong University of Traditional Chinese Medicine
Wenjun Jiang
Shandong Provincial Key Laboratory of Integrated Traditional Chinese and Western Medicine for Prevention and Therapy of Ocular Diseases
Guoli Zhang
Shandong Tumor Hospital & Intitute
Weiming Zhu
First Teaching Hospital of Tianjin University of Traditional Chinese Medicine
Xin Li
Affiliated Hospital of Shandong University of Traditional Chinese Medicine
Xueyun Pang
Juxian Hospital of Traditional Chineses Medicine
Wei Liu (lw_1369@163.com)
Second Affiliated Hospital of Shandong University of Traditional Chinese Medicine

Research Article

Keywords: Cerebral Ischemic Stroke (CIS), Corticospinal tract remodeling, Slits, Robos

Posted Date: September 8th, 2021

DOI: https://doi.org/10.21203/rs.3.rs-170440/v1

Version of Record: A version of this preprint was published at Molecular Biology Reports on October 15th, 2021. See the published version at https://doi.org/10.1007/s11033-021-06803-1.

Abstract

Background: Slits and Robos were associated with the generation of axons of corticospinal tract during the corticospinal tract (CST) remodeling after the cerebral ischemic stroke (CIS). However, little is known about the mechanism of CST remodeling. In this study, we detected the expression of Slits and Robos in middle cerebral artery occlusion (MCAO) rats to investigate the roles of Slits and Robos in the CIS.

Methods: MCAO model was established using modified Zea Longa method. Beam walking test (BWT) was conducted to evaluate the motor function. The images of the track of cortical spinal cord beam on day 7, 14 and 21 were observed by anterograde CST tracing. Biopinylated dextan amine (BDA) was used to mark CST anterogradely. Expression of *GAP-43* mRNA and GAP-43 protein in cervical spinal cord was detected by Real-Time PCR and Western blot analysis, respectively. The expression of Slit1, Slit2 and Robo1 in cervical spinal cord was detected by immunofluorescence staining.

Results: The scores in the model group were significantly reduced compared to sham-operation group on day 7 ($P<0.001$), 14 ($P<0.001$) and 21 ($P<0.001$), respectively. There was no significant difference in the score on day 7, 14 and 21 of the sham-operation groups ($P>0.05$). In contrast, significant increase was noticed in the scores in model group, presenting a time-dependent manner. More CST staining fibers could be observed at the degenerative side in the model group compared with that of the sham-operation group on day 21. *GAP-43* mRNA expression in the model group showed significant increase compared to that of sham-operation group on day 14 ($P=0.015$) and 21 days ($P=0.002$). The expression of GAP-43 protein in model group showed significant increase compared to that of sham-operation group on day 14 ($P=0.022$) and day 21 ($P=0.008$), respectively. The expression of Slit1 and Slit2 showed increase on day 14 and day 21, while the expression of Robo1 showed significant decrease in MCAO rats.

Conclusion: Up-regulation of Slit1 and Slit2 and the downregulation of Robo1 may be related to the axons of CST midline crossing in spinal cord of MCAO rat during the spontaneous recovery of impaired motor function.

Background

Cerebral ischemic stroke (CIS), one of the most serious diseases threatening the health of human beings [1, 2], is defined as ischemic necrosis or cerebromalacia induced by disorder of cerebral blood or hypoxia accompanied by neurological function defect such as motor dysfunction. Remodeling of corticospinal tract (CST) is considered a key event for the recovery of motor function after CIS [3]. Under normal conditions, axons of CST were localized at the preliminary sites and were inhibited to pass through the midline of the spinal cord. Nevertheless, in the presence of CIS, axons of CST that stemmed from the intact cortex could pass through the midline of spinal cord, which involved in the reconstruction of neural network of the damaged sites after CIS.

Slits (i.e. Slit 1-3) and Robo receptors (i.e. Robo1-4) are crucial for the passing of axons through the midline of spinal cord that is closely related to the CST. Indeed, the Slit-Robo signaling had been

confirmed to participate in the autocrine/juxtaparacrine regulation of axon fasciculation. For example, co-expression of *Slit* and *glypican-1* mRNA was found in the reactive astrocytes of the injured adult brain tissues [4]. In focal cerebral infarction rats, electroacupuncture intervention significantly improved the neurological function and obviously upregulated the expression of cerebral Slit 2 and Robo 1 proteins [5]. Moreover, expression of netrin-1, Slit-1 and Slit-3 but not of Slit-2 was detected in cerebellar and spinal cord lesions [6]. Nevertheless, the roles of Slit-Robo signaling pathway in the focal cerebral infarction are still not well defined.

GAP43, a nervous tissue specific protein, is highly expressed in neurons during development and nerve regeneration. As is known to all, GAP43 is implicated in neural axon outgrowth, long-term potentiation, signal transduction, and neurotransmitter release. In the presence of neural damages, GAP43 is highly expressed. This led us to investigate the roles of GAP43 in the pathogenesis of CIS.

In this study, we aimed to investigate the expression of Slit1, Slit2 and Robo1 expression in the cervical cord midline in the rats with focal cerebral infarction. Specifically, we detected the expression of Slit1, Slit2 and Robo1 during the process of CST remodeling in cervical spinal cord in MCAO rats.

Materials And Methods

Animals

Forty-eight adult male Sprague Dawley (SD) rats (250-300 g; certificate No.: SCXK Lu 2014-0007) were provided by Lukang Pharmacy (Linyi, China). The rats were kept in a controlled environment at a constant temperature of 25±1˚C and a humidity of 50%±10%. All the animals were free access to food and water on a 12h/12 h light/dark cycle for at least 21 days under standard conditions before any treatment.

MCAO construction

MCAO was established according to Zea-Longa's method, with slight modifications [7]. In brief, the rats were intraperitoneally anesthetized with 4% chloral hydrate (0.7 ml/100 g). Then the anterior cervical tissues were cut longitudinally to expose the right common carotid artery (CCA), external carotid artery (ECA) and internal carotid artery (ICA). A small incision was made at a position that was about 4 mm from the CCA branch, and then a line was inserted into the blood vessel at a depth of 18 mm.

Experimental design

The rats were randomly divided into sham-operation group (n=24) and the MCAO model group (n=24), according to the random number table method. The rats in the sham-operation group were given a ligation of right carotid artery without inserting the line. In the model group, MCAO induction was conducted on day 1. BDA injection was performed in both groups on day 7, together with behavioral tests on day 7, 14 and 21, respectively. Animals were sacrificed on day 7, 14 and 21, followed by sample collection for the subsequent tests, including immunohistochemistry, Western blot analysis, and Real-Time PCR.

Neurobehavioral Evaluation

Behavioral testing was performed by experienced investigators blinded to the experimental groups. The performance of animals in behavioral tests was assessed during the light portion of the light-dark cycle. The methods for each behavioral test are listed as follows.

The beam walking test

To evaluate the motor function of rats, the beam walking test (BWT) was conducted on day 7, 14 and 21 according to the previous description [8]. Briefly, rats were placed on a beam with a size of 122 cm×2.5 cm×75.5 cm, and were trained to walk along the beam to reach the opposite side of the beam for three trials about 3 days before the experiment [9]. A 0 to 7-point scale modified from Goldstein method [10] was utilized to evaluate the locomotor function of the animals.

The modified grip-traction test

The rats were required to grasp a plastic tube placed in an horizontal direction (0.6 cm in diameter) with their forward claws. The tube was about 45 cm above a desk. Then we determined the muscle strength and recorded the time for falling.

The rotarod test

Three days before MCAO induction, the rats were trained on a rotated bar (4-35 rotation per min). All the animals were trained for 3 days, with a frequency of 3 times per day lasting for 5 min, respectively. Then we recorded the time of animals with no falling when walking on the rotated bar. The time interval for the test was 15 min. The averaged value was obtained after two tests.

Anterograde corticospinal tract tracing

Biotinylated dextan amine (BDA, 0.2 μl) was injected to 4 sites. For the selection of injection sites, two sites were fixed in the position that was about 1 mm and 2 mm from the anterior and posterior bregma, while two sites were fixed in the position that was about 3.5 mm and 4 mm to the lateral bregma. After deep anesthesia, the rats were positioned on a stereotaxic apparatus via a finely drawn glass capillary on day 7. For each site, the BDA was injected at a depth of 1.5 mm, and the needles were dwelled for 2 min after injection.

Two weeks after BDA injection, rats were anesthetized and sacrificed for the subsequent analysis. Cervical spinal cord tissues obtained from C4-C6 segments were fixed by 4% paraformaldehyde overnight, followed by dehydration in sucrose with a concentration of 10%, 20% and 30%, respectively. The tissues were then embedded by paraffin, and the sections (7 μm) were placed in 0.5% H_2O_2 for 15 min, followed by washing three times with tris-buffered saline (TBS) solution. Subsequently, the sections were incubated in TBS containing 0.3% Trition X-100 at 4˚C for 6 h, and then were incubated overnight

with HRP. The sections were presented in DAB solution for 15 min and were attached to the antistripping slide. Finally, the images were observed by light microscope.

Quantitative Real-Time PCR

Total RNA was extracted from the tissues of the left cervical spinal cords using TRIzol reagent (Thermo Fisher Scientific, CA, USA). The cDNA synthesis was carried out using the Transcriptor First-Strand cDNA Synthesis kit (Roche Diagnostics, Basel, Switzerland). Quantitative PCR was performed using 2 × SYBR Green qPCR Mix (Aid lab Biotech, Beijing, China). PCR amplification was performed using a Real-Time PCR System (Agilent Tech, CA, USA) using the following specific primers: β-actin, 5'-GCCTTCCTTCCTGGGTATGG-3', 5'-ACGCAGCTCAGTAACAGTCC-3'; GAP-43, 5'-ACCACTGATAACTCGCCGTC-3', 5'-CTACAGCTTCTTTCTCCTCCTC-3'. The amplification conditions were as follows: denaturation at 94˚C for 5 min, 42 cycles at 95˚C for 10 sec, 58˚C for 30 sec, and 72˚C for 30 sec. The amplification results were evaluated using the ΔΔCq method as previously described [11].

Western blot analysis

Protein was extracted from the left cervical spinal cord homogenized in RIPA lysis buffer. The protein concentration was evaluated based on BCA method, followed by separation by 10% SDS–PAGE gels. Afterwards, proteins were transferred onto polyvinylidene difluoride membranes under 80 V for 30min and 100V for 2 h. The membranes were blocked with 5% non-fat dry milk for 1 h and incubated at 4˚C overnight with primary rabbit anti-GAP-43 (1:20,000, Abcam, UK). Then the membranes were incubated with secondary antibody, goat anti-rabbit IgA (1:3,000, Bioss, Beijing, China), for 1 h at room temperature. The beta-actin served as the internal standard. Finally, the band gray values were analyzed via the application of Bio1D software.

Immunofluorescence

Cervical spinal cord tissue sections (6 μm) were soaked in acetone for 15 min and were incubated with 10% goat serum (0.01 mmol/L) at room temperature for 1 h. The slices were incubated with primary antibody overnight at 4˚ C, including mouse anti-Slit1 (1: 100, Abcam), rabbit anti-Slit2 (1: 100, Abcam), and rabbit anti-Robo1 (1: 10, Abcam). Upon washing with PBS, the slices were incubated with secondary antibodies at room temperature for 2 h, including Alexa Fluor488-conjugated goat anti-rabbit IgG (1:400; H&L, ab150077), Alexa Fluor 555-conjugated goat anti-mouse IgG (1:400; H&L, ab150114). DAPI solution (1:500) was added to the slices. After fluorescence quenching, the images were observed under a fluorescence microscope (ZEISS 780).

Statistical analysis

SPSS 18.0 (SPSS, Chicago, USA) was utilized for the data analysis. All the data were expressed as mean ± standard error of mean. Student's t-test or the Mann–Whitney test was used for the comparison of measurement data between the two groups. $P < 0.05$ was statistically significant.

Results

Neurological functional outcome and lesion volume

For the neurological function evaluation, the scores obtained based on Goldstein method in the model group showed significant decline compared to that of sham-operation group on day 7 (P<0.001), day 14 (P<0.001), and day 21 (P<0.001), respectively (Fig1a, paired sample t-test). No significant differences were noticed in the scores on day 7, 14 and 21 in the sham-operation group (P>0.05, Fig1a). By contrast, significant increase was noticed in the scores in model group, presenting a time-dependent manner. Compared with sham control, the grip-traction time on day 7, 14 and 21 showed significant decline in the MCAO group (P<0.05, Fig1b). The residual time on rod in the MCAO group was significantly shorter on day 7, 14 and 21 compared with the sham control (P<0.05). With the time went on, the residual time on rod in the MCAO group showed significant increase on day 7, 14 and 21 (P<0.05, Figure 1c). TTC staining showed that the infarction size showed significant decrease on day 14 and day 21 compared with that on day 7 (P<0.05, Figure 1d and 1e). This implied that motor function in MCAO rats showed significant reduction after surgery compared to that of sham-operation group. Nevertheless, these tests indicated that the motor function of MCAO rats could spontaneously recovered to some extent.

Midline-crossing CST axon sprouted into the denervated side of the cervical cord

About 14 days after injection, BDA was traced at CST of cervical spinal cord in sham-operation group and model group, respectively (Fig2a and 2c). In addition, more fibers stained in the CST region were available in the model group compared with the sham-operation group on day 21 (Fig2b and 2d). This implied that axons of CST could pass through the midline and entered the denervated side on day 21.

Expression of GAP-43 in the cervical spinal cord

In the model group, expression of *GAP-43* mRNA showed significant increase compared to that of sham-operation group on day 14 (P=0.015) and day 21 (P=0.002), respectively (Fig3a). Similarly, expression of GAP-43 protein in model group showed significant up-regulation compared to that of sham-operation group on day 14 (P=0.022) and day 21 (P=0.008) (Fig3b and 3c). This implied that the CST axons in the denervated side remodeling on day 14, which lasted until day 21.

Immunohistochemical staining of Slit1, Slit2 and Robo1 in the cervical spinal cord

The protein expression of Robo1 was significantly down-regulated as revealed by immunohistochemical staining. Meanwhile, the expression of Slit1 and Slit2 protein was significantly up regulated in the model group on day 14 and day 21 (Fig4-6). By contrast, compared with the sham-operation group, there was no significant differences for the expression of Slit1, Slit2 and Robo1 on day 7 in the model group (P>0.05). On this basis, Slit1, Slit2 and Robo1 were involved in the process of CST remodeling after the surgery.

Discussion

CIS is the most common cause for long-term disability in adults [12, 13], and most of the patients (approximately 75%) show various motor dysfunction [14]. According to the previous description, there was CST axonal loss in MCAO rats [15]. CST is a beam linked the sensorimotor cortex and the ventral horn motor neuron in spinal cord, which dominates the voluntary movement of skeletal muscle. In cases of CIS, there would be loss of domination of cortex for the contralateral motor neuron, which subsequently led to deficiency of contralateral motor function and a spastic paralysis. In a previous study, Murphy and Corbett reported spontaneous improvement of motor function in MCAO rats after CIS surgery [16]. Meanwhile, CST could pass through the midline of spinal cord to form new synapses of motor unit in the denervated side to promote the recovery of motor function in animal models with cerebral injury [17]. Therefore, the remodeling of CST axons promoted the CST midline passing through the denervated side, which was vital for spontaneous motor function recovery in CIS patients.

GAP-43 has been well acknowledged as a marker for axon growth. As a unique membrane-associated protein, it played crucial roles in the development and remodeling of the neurons. GAP-43 protein used for the labeling of axonal growth is mainly expressed at the regenerated axonal terminal [18-20]. Previously, up-regulation of GAP-43 was associated with the motor function recovery in both brain and spinal cord injury animal models [21-23]. In our study, the motor function recovery can be observed in the model group. In addition, the expression of both *GAP-43* mRNA and GAP-43 protein in the model group showed significant increase after surgery on day 14 and day 21 compared with the sham-operation group, demonstrating the presence of the CST remodeling in MCAO rats at the denervated sides. BDA stained CST axons were found at the denervated side on day 21 after modeling, which showed that the CST axons presented at the denervated side were derived from the innervated side. This process mainly occurred on day 21 after surgery.

Nowadays, extensive studies have focused on the roles of Slit1, Slit2 and Robo1 in the nervous system. For instance, Slit1 was merely expressed in nervous system, while Slit2 was expressed mainly in nerve tissues. Robo1 was expressed in the central nervous system of mammalians and was uniformly distributed in axon. Besides, Robo1 could bind to all Slits proteins [24], which could be expressed by motor neurons [25, 26]. Our finding suggested that the up-regulation of Slits and down-regulation of Robo may activate the CST midline crossing upon the sprouting of the axons at the innervated side of spinal cord in MCAO rats. This indicated that up-regulation of Slits and/or down-regulation of Robos might prompt motor recovery after CIS.

In the process of CST remodeling, the midline repulsion contains two courses: guiding the axons to cross the midline; and preventing the axons from re-crossing the midline once they crossed or under normal conditions. The Slit-Robo signaling pathway seemed to be activated in both of these processes. Slit-Robo pathway, acting as a signaling of repulsion, was imperative for maintaining the ipsilateral axon pathways under normal conditions [27-29]. In a previous study, Slit-Robo pathway played a key role in guiding dorsally projecting cranial motoneurons and facilitating the exit of neural tube [30]. Robo1 receptor could respond to Slits in spinal motor axons, which thereby repelling axons in vivo and in vitro [25, 31, 32]. Such repulsive reaction might be related to a self-silencing mechanism [33]. Suppressing the

expression of Robo1 can promote axon outgrowth and midline crossing, while over-expression of Robo1 repelled the axons from the midline and prevented their re-crossing [34-36]. Similarly, our data showed that Robo1 was downregulated in MCAO rats in the presence of axons at the denevated side of cervical spinal cord.

To our best knowledge, Slit1, Slit2 and Robo1 could regulate the CST remodeling process in the spinal cord, however, there are still some disputes on the expression pattern. Liu [37] reported that the Slit2 expression began to raise about 7 days after spinal cord injury (SCI), and reached the peak level on day 14. However, the receptor Robo1 showed no significant changes at all time points, which indicated that Slit2-Robo1 signal pathway did not involve in the CST remodeling after SCI. In our study, the expression of Slit1 and Slit2 showed significant increase after surgery on day 7. In a previous study, Li et al [38] indicated that 48 hours following SCI in rats, up-regulation of Slit2 and down-regulation of Robo1 hindered the CST remodeling in spinal cord. Our findings were on the contrary, which might imply that Slits and Robos exerted different roles in different time point, and the animal model could also be a possible cause for it.

Indeed, there are some limitations in our study. We could not illustrate the exact mechanism of how Slit1, Slit2, Robo1, and GAP43 in the pathogenesis of CIS, despite we presented their changes in the MCAO rats. In future, more studies involving the silencing of Slit1, Slit2, Robo1, and GAP43 are required to further illustrate their exact roles in the CIS.

Conclusion

In summary, the CST remodeling occurred with the spontaneous motor function recovery from 14 days to 21 days after MCAO. This was associated with the downregulation of Robo1 and up-regulation of Slit1 and Slit2.

Abbreviations

MCAO, middle cerebral artery occlusion; CIS, cerebral ischemic stroke; CST, corticospinal tract; CCA, common carotid artery; ECA, external carotid artery; ICA, internal carotid artery; BWT, beam walking test; BDA, biotinylated dextran amine

Declarations

Funding

This study was supported by National Natural Science Foundation of China (No.81273701), and Natural Science Foundation of Shandong Province (No. ZR2019MH056).

Competing interests

All the authors declare that they have no competing interests.

Availability of data and materials

The raw data supporting the conclusions of this manuscript will be made available by the authors, without undue reservation, to any qualified researcher.

Ethics approval

All experiments were approved by the Laboratory Animal Care and Use Committee of Shandong University of Traditional Chinese Medicine (No. 2014-0104).

Authors' Contributions

JX Wu: data analysis and interpretation, wrote the manuscript; WJ Jiang: statistical analysis, drafting the manuscript; GL Zhang: prepared the study, data interpretation, and a major contributor in writing the manuscript; ZH Ying: animal model establishing, critical revision of the manuscript; X Li: data analysis and interpretation, critical revision on the manuscript; XY Pang: data analysis and interpretation, a major contributor in writing the manuscript; W Liu: data analysis and interpretation and was a major contributor in writing the manuscript. All authors have read and approved the final version of the manuscript.

Acknowledgements

Not applicable.

References

1. Hsing WT, Imamura M, Weaver K, Fregni F, Azevedo Neto RS (2012) Clinical effects of scalp electrical acupuncture in stroke: a sham-controlled randomized clinical trial. J Altern Complement Med 18(4):341-346. doi: 10.1089/acm.2011.0131.
2. Zhang C, Wen Y, Fan X, Yang S, Tian G, Zhou X, Chen Y, Meng Z (2015) A microarray study of middle cerebral occlusion rat brain with acupuncture intervention. Evid Based Complement Alternat Med 2015:496932. doi: 10.1155/2015/496932.
3. DeVetten G, Coutts SB, Hill MD, Goyal M, Eesa M, O'Brien B, Demchuk AM, Kirton A (2010) Acute corticospinal tract Wallerian degeneration is associated with stroke outcome. Stroke 41(4):751-756. doi: 10.1161/strokeaha.109.573287.
4. Hagino S, Iseki K, Mori T, Zhang Y, Hikake T, Yokoya S, Takeuchi M, Hasimoto H, Kikuchi S, Wanaka A (2003) Slit and glypican-1 mRNAs are coexpressed in the reactive astrocytes of the injured adult brain. Glia 42(2):130-138. doi: 10.1002/glia.10207.
5. Lü K, Li F, Gong B, Dai EZ, Wang Y, Zeng ZH (2013) [Effect of electroacupuncture of "Neiguan" (PC 6) and "Zusanli" (ST 36) on expression of cerebral cortical slit 2/Robo 1 in the focal cerebral infarction rats]. Zhen Ci Yan Jiu 38(4):265-270.

6. Wehrle R, Camand E, Chedotal A, Sotelo C, Dusart I (2005) Expression of netrin-1, slit-1 and slit-3 but not of slit-2 after cerebellar and spinal cord lesions. Eur J Neurosci 22(9):2134-2144. doi: 10.1111/j.1460-9568.2005.04419.x.
7. Longa EZ, Weinstein PR, Carlson S, Cummins R (1989) Reversible middle cerebral artery occlusion without craniectomy in rats. Stroke 20(1):84-91. doi: 10.1161/01.str.20.1.84.
8. Watson GpC (2005) Atlas of stereotaxy of rat brain. Beijing: people's health press, first edition.
9. Schaechter JD, Fricker ZP, Perdue KL, Helmer KG, Vangel MG, Greve DN, Makris N (2009) Microstructural status of ipsilesional and contralesional corticospinal tract correlates with motor skill in chronic stroke patients. Hum Brain Mapp 30(11):3461-3474. doi: 10.1002/hbm.20770.
10. Goldstein LB (1997) Effects of bilateral and unilateral locus coeruleus lesions on beam-walking recovery after subsequent unilateral sensorimotor cortex suction-ablation in the rat. Restor Neurol Neurosci 11(1):55-63. doi: 10.3233/rnn-1997-111206.
11. Mazzei M, Vascellari M, Zanardello C, Melchiotti E, Vannini S, Forzan M, Marchetti V, Albanese F, Abramo F (2019) Quantitative real time polymerase chain reaction (qRT-PCR) and RNAscope in situ hybridization (RNA-ISH) as effective tools to diagnose feline herpesvirus-1-associated dermatitis. Vet Dermatol 30(6):491-e147. doi: 10.1111/vde.12787.
12. Lakhan SE, Kirchgessner A, Hofer M (2009) Inflammatory mechanisms in ischemic stroke: therapeutic approaches. J Transl Med 7:97. doi: 10.1186/1479-5876-7-97.
13. Singh A, Jenkins C, Calys-Tagoe B, Arulogun OS, Sarfo S, Ovbiagele B, Akpalu A, Melikam S, Uvere E, Owolabi MO (2017) Stroke Investigative Research and Education Network: Public Outreach and Engagement. J Community Med Health Educ 7(2). doi: 10.4172/2161-0711.1000518.
14. Liu M, Wu B, Wang WZ, Lee LM, Zhang SH, Kong LZ (2007) Stroke in China: epidemiology, prevention, and management strategies. Lancet Neurol 6(5):456-464. doi: 10.1016/s1474-4422(07)70004-2.
15. Dang G, Chen X, Chen Y, Zhao Y, Ouyang F, Zeng J (2016) Dynamic secondary degeneration in the spinal cord and ventral root after a focal cerebral infarction among hypertensive rats. Sci Rep 6:22655. doi: 10.1038/srep22655.
16. Murphy TH, Corbett D (2009) Plasticity during stroke recovery: from synapse to behaviour. Nat Rev Neurosci 10(12):861-872. doi: 10.1038/nrn2735.
17. Oshima T, Lee S, Sato A, Oda S, Hirasawa H, Yamashita T (2009) TNF-alpha contributes to axonal sprouting and functional recovery following traumatic brain injury. Brain Res 1290:102-110. doi: 10.1016/j.brainres.2009.07.022.
18. Holahan MR (2017) A Shift from a Pivotal to Supporting Role for the Growth-Associated Protein (GAP-43) in the Coordination of Axonal Structural and Functional Plasticity. Front Cell Neurosci 11:266. doi: 10.3389/fncel.2017.00266.
19. Bird CW, Gardiner AS, Bolognani F, Tanner DC, Chen CY, Lin WJ, Yoo S, Twiss JL, Perrone-Bizzozero N (2013) KSRP modulation of GAP-43 mRNA stability restricts axonal outgrowth in embryonic hippocampal neurons. PLoS One 8(11):e79255. doi: 10.1371/journal.pone.0079255.

20. Yang P, Wen H, Ou S, Cui J, Fan D (2012) IL-6 promotes regeneration and functional recovery after cortical spinal tract injury by reactivating intrinsic growth program of neurons and enhancing synapse formation. Exp Neurol 236(1):19-27. doi: 10.1016/j.expneurol.2012.03.019.
21. Liu F, Liao F, Li W, Han Y, Liao D (2014) Progesterone alters Nogo-A, GFAP and GAP-43 expression in a rat model of traumatic brain injury. Mol Med Rep 9(4):1225-1231. doi: 10.3892/mmr.2014.1967.
22. Liu GM, Luo YG, Li J, Xu K (2016) Knockdown of Nogo gene by short hairpin RNA interference promotes functional recovery of spinal cord injury in a rat model. Mol Med Rep 13(5):4431-4436. doi: 10.3892/mmr.2016.5072.
23. Zhao S, Zhao M, Xiao T, Jolkkonen J, Zhao C (2013) Constraint-induced movement therapy overcomes the intrinsic axonal growth-inhibitory signals in stroke rats. Stroke 44(6):1698-1705. doi: 10.1161/strokeaha.111.000361.
24. Long H, Sabatier C, Ma L, Plump A, Yuan W, Ornitz DM, Tamada A, Murakami F, Goodman CS, Tessier-Lavigne M (2004) Conserved roles for Slit and Robo proteins in midline commissural axon guidance. Neuron 42(2):213-223. doi: 10.1016/s0896-6273(04)00179-5.
25. Kim M, Fontelonga T, Roesener AP, Lee H, Gurung S, Mendonca PRF, Mastick GS (2015) Motor neuron cell bodies are actively positioned by Slit/Robo repulsion and Netrin/DCC attraction. Dev Biol 399(1):68-79. doi: 10.1016/j.ydbio.2014.12.014.
26. Lee H, Kim M, Kim N, Macfarlan T, Pfaff SL, Mastick GS, Song MR (2015) Slit and Semaphorin signaling governed by Islet transcription factors positions motor neuron somata within the neural tube. Exp Neurol 269:17-27. doi: 10.1016/j.expneurol.2015.03.024.
27. Howard LJ, Brown HE, Wadsworth BC, Evans TA (2019) Midline axon guidance in the Drosophila embryonic central nervous system. Semin Cell Dev Biol 85:13-25. doi: 10.1016/j.semcdb.2017.11.029.
28. Bjorke B, Shoja-Taheri F, Kim M, Robinson GE, Fontelonga T, Kim KT, Song MR, Mastick GS (2016) Contralateral migration of oculomotor neurons is regulated by Slit/Robo signaling. Neural Dev 11(1):18. doi: 10.1186/s13064-016-0073-y.
29. Brown HE, Reichert MC, Evans TA (2015) Slit Binding via the Ig1 Domain Is Essential for Midline Repulsion by Drosophila Robo1 but Dispensable for Receptor Expression, Localization, and Regulation in Vivo. G3 (Bethesda) 5(11):2429-2439. doi: 10.1534/g3.115.022327.
30. Hammond R, Vivancos V, Naeem A, Chilton J, Mambetisaeva E, Andrews W, Sundaresan V, Guthrie S (2005) Slit-mediated repulsion is a key regulator of motor axon pathfinding in the hindbrain. Development 132(20):4483-4495. doi: 10.1242/dev.02038.
31. Kim M, Fontelonga TM, Lee CH, Barnum SJ, Mastick GS (2017) Motor axons are guided to exit points in the spinal cord by Slit and Netrin signals. Dev Biol 432(1):178-191. doi: 10.1016/j.ydbio.2017.09.038.
32. Bai G, Chivatakarn O, Bonanomi D, Lettieri K, Franco L, Xia C, Stein E, Ma L, Lewcock JW, Pfaff SL (2011) Presenilin-dependent receptor processing is required for axon guidance. Cell 144(1):106-118. doi: 10.1016/j.cell.2010.11.053.

33. Bacon C, Endris V, Rappold GA (2013) The cellular function of srGAP3 and its role in neuronal morphogenesis. Mech Dev 130(6-8):391-395. doi: 10.1016/j.mod.2012.10.005.
34. Ypsilanti AR, Zagar Y, Chédotal A (2010) Moving away from the midline: new developments for Slit and Robo. Development 137(12):1939-1952. doi: 10.1242/dev.044511.
35. Dickson BJ, Gilestro GF (2006) Regulation of commissural axon pathfinding by slit and its Robo receptors. Annu Rev Cell Dev Biol 22:651-675. doi: 10.1146/annurev.cellbio.21.090704.151234.
36. Yang T, Huang H, Shao Q, Yee S, Majumder T, Liu G (2018) miR-92 Suppresses Robo1 Translation to Modulate Slit Sensitivity in Commissural Axon Guidance. Cell Rep 24(10):2694-2708.e2696. doi: 10.1016/j.celrep.2018.08.021.
37. Liu JB, Jiang YQ, Gong AH, Zhang ZJ, Jiang Q, Chu XP (2011) Expression of Slit2 and Robo1 after traumatic lesions of the rat spinal cord. Acta Histochem 113(1):43-48. doi: 10.1016/j.acthis.2009.08.003.
38. Li Y, Gao Y, Xu X, Shi R, Liu J, Yao W, Ke C (2017) Slit2/Robo1 promotes synaptogenesis and functional recovery of spinal cord injury. Neuroreport 28(2):75-81. doi: 10.1097/wnr.0000000000000715.

Figures

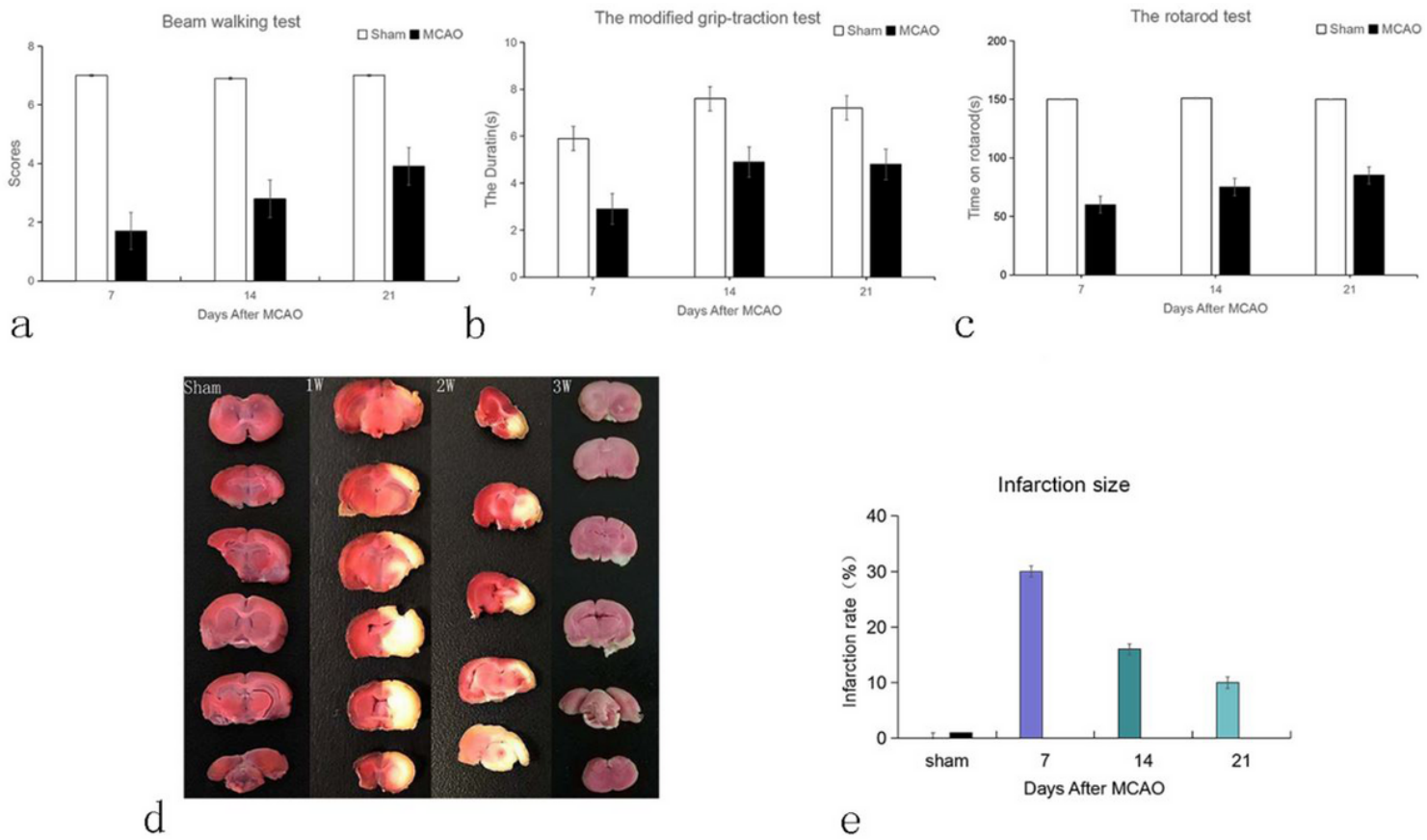

Figure 1

Motor function and cerebral infarction size at the corresponding time point. The motor function was determined using beam walking test (a), the modified grip-traction test (b) and rotarod test (c). The infarction size was evaluated using the TTC staining. Infarction size in each group (d). Infarction rate in each group (e). Data were represented as mean ± standard error of mean (SEM). n = 24; *P<0.05 vs. model group.

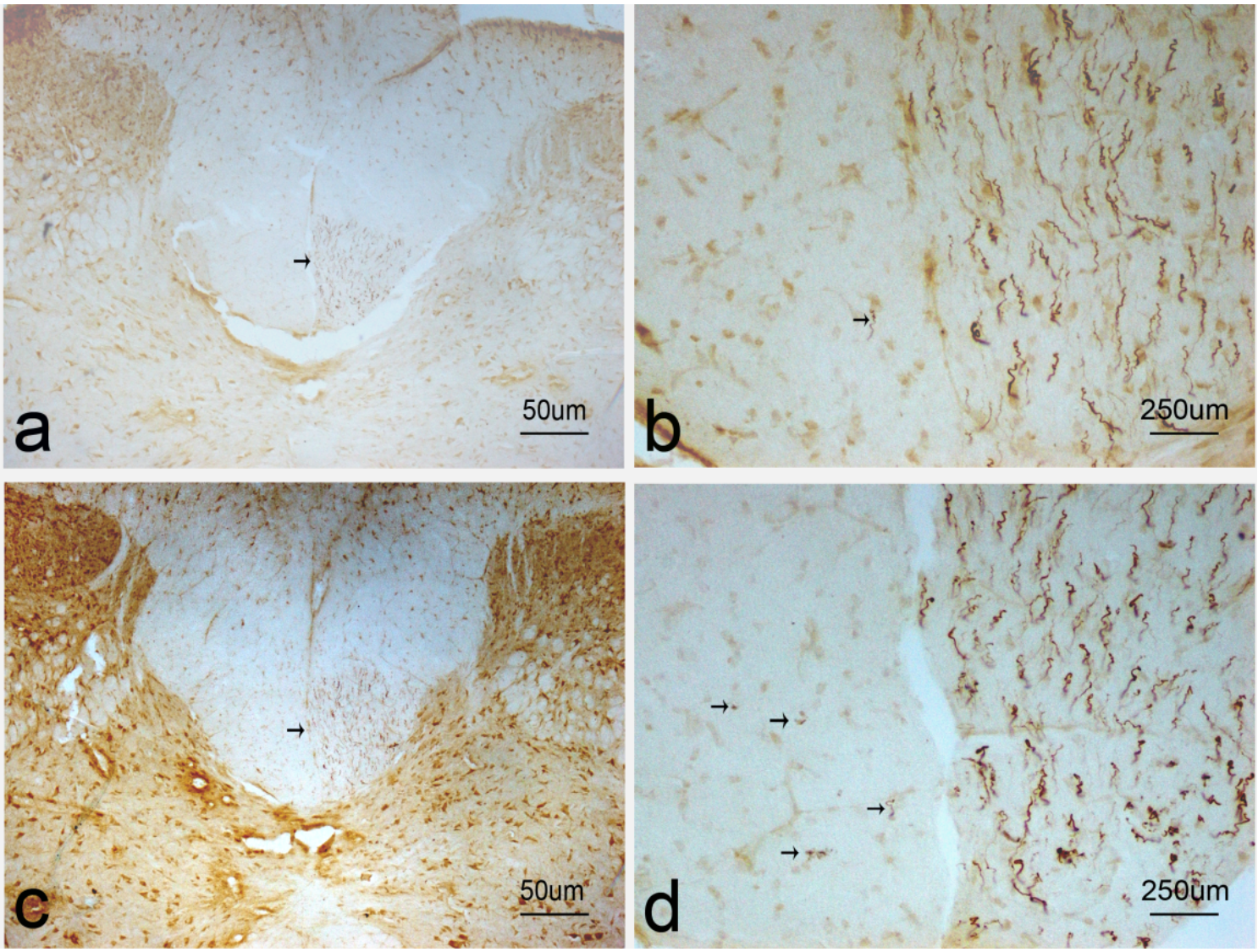

Figure 2

The axons were presented at the innervated side on day 21. The arrow indicated the BDA labeled corticospinal tract fibers. (a, b) the sham-operation group. (c, d) model group. The images were observed under a magnification of 40× (a and c), and 200× (b and d).

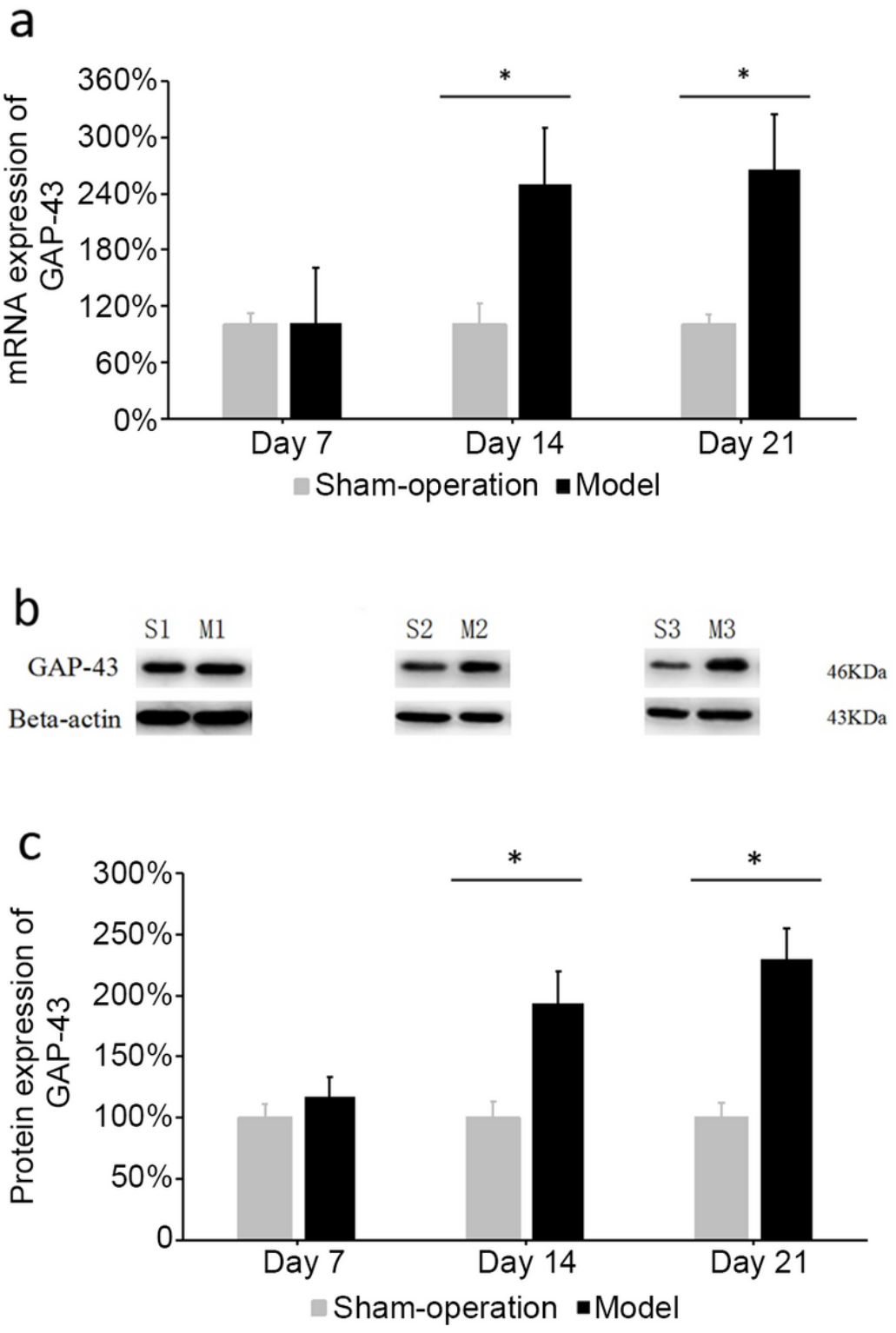

Figure 3

The mRNA and protein expression of GAP-43 in left cervical spinal cord. (a) GAP-43 mRNA expression. (b) GAP-43 protein expression. S1, S2, S3 represented sham-operation group on day 7, 14, and 21, respectively. M1, M2, M3 represented model group on day 7, 14, and 21, respectively. (c) Protein expression of GAP-43. Data were represented as mean ± SEM, n = 3; *P< 0.05.

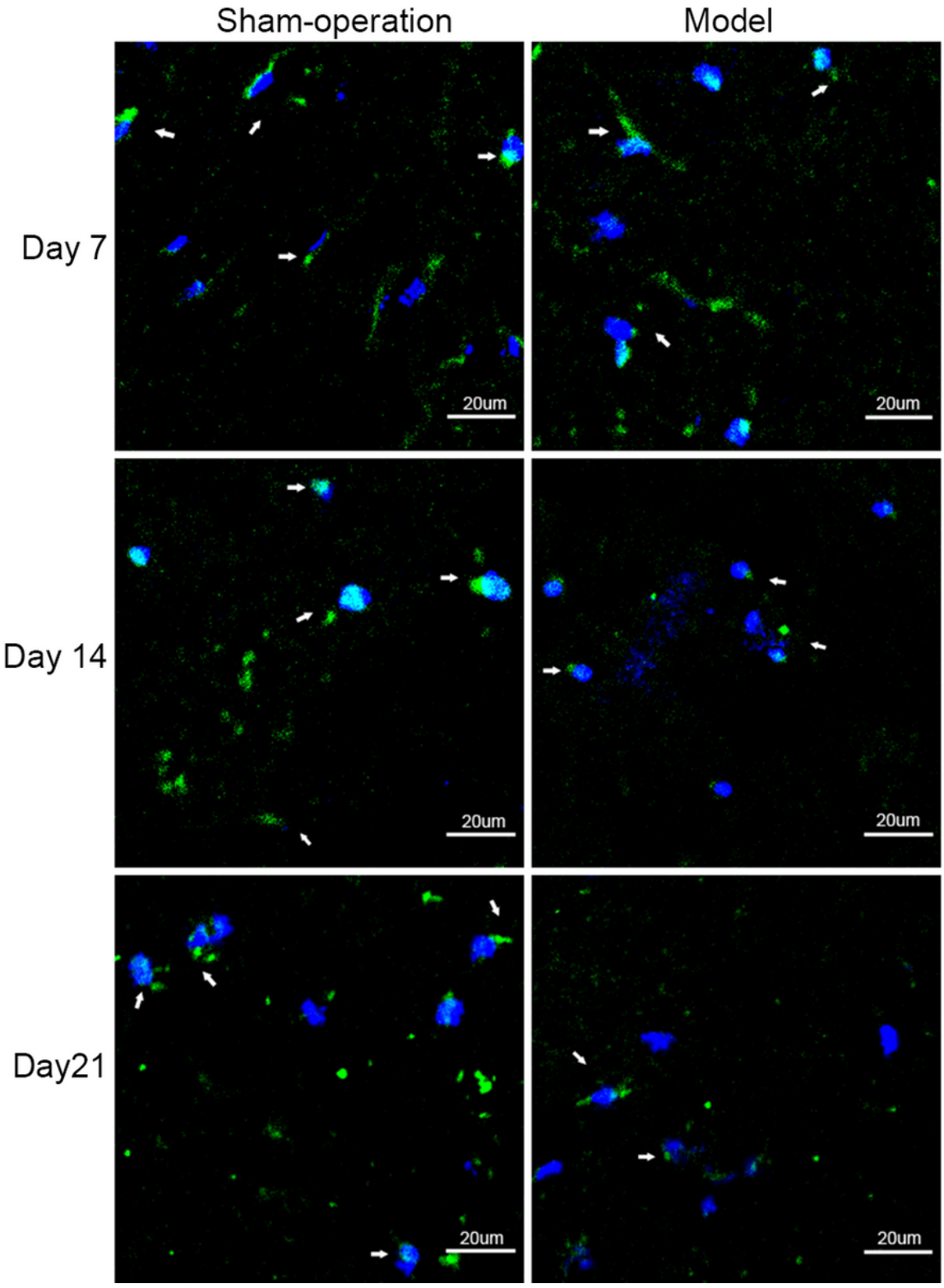

Figure 4

Robo1 expression after positioning analysis using immunohistochemical staining. The fluorescence intensity labeled blue color indicates nuclei that were stained with DAPI, and green color showed the localization of robo1 protein. The arrow indicated robo1 protein. The images were observed under a magnification of 200×.

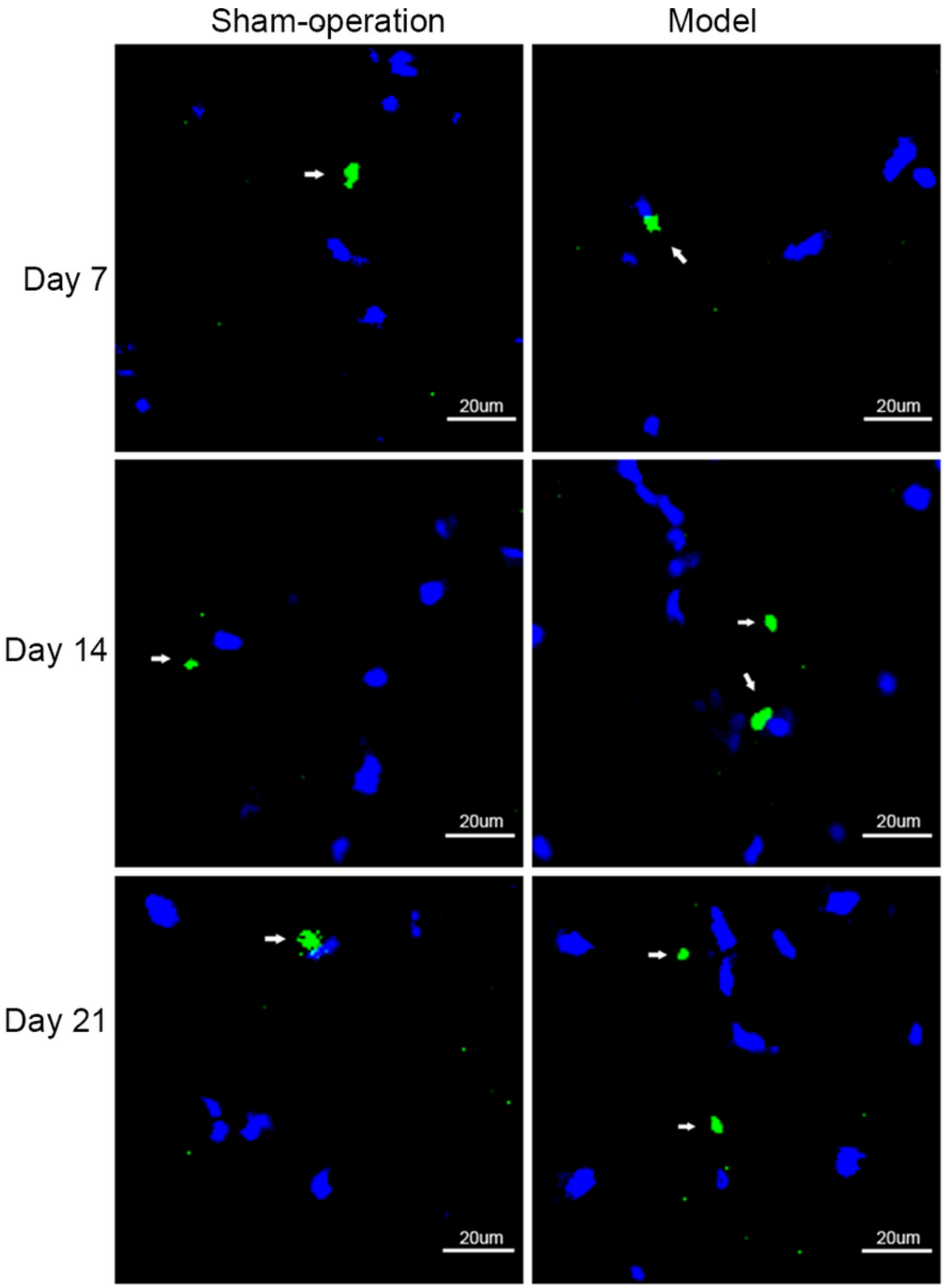

Figure 5

Slit1 expression on day 7, 14 and 21 based on positioning analysis using immunohistochemical staining. The fluorescence intensity labeled blue color indicates nuclei that were stained with DAPI, and green color indicated the localization of Slit1 protein. The arrow indicated Slit1 protein. The images were observed under a magnification of 200×.

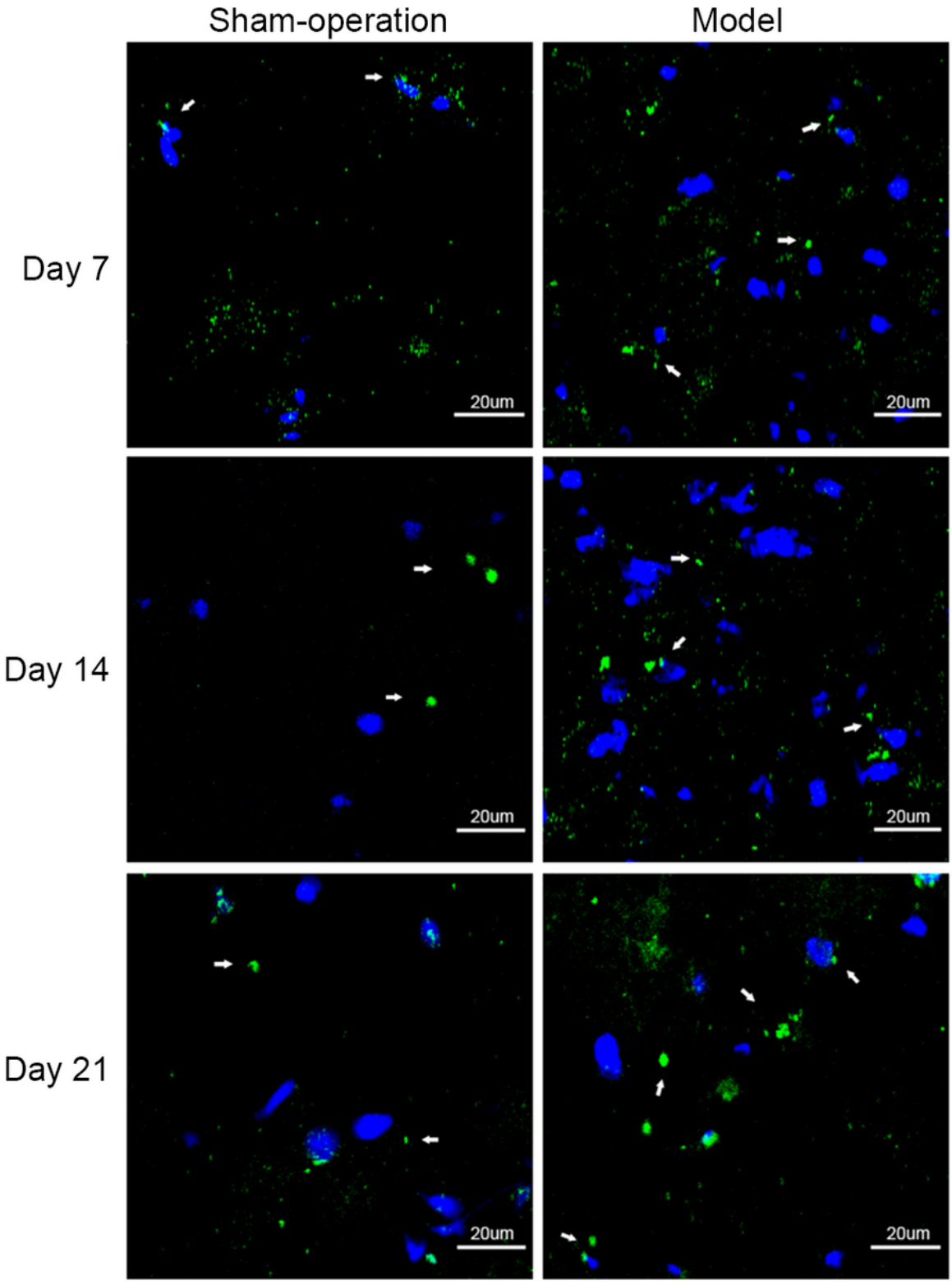

Figure 6

Slit2 expression based on positioning analysis using immunohistochemical staining. The green color showed the localization of Slit2 protein. The arrow indicated the Slit2 protein. The images were observed under a magnification of 200×.